Journal of Magnetic Resonance **138,** 123–126 (1999)
Article ID jmre.1999.1724, available online at http://www.idealibrary.com on IDEAL®

Reconstructing Powder NQR Images with Real Gradient Coils

Srirama V. Swaminathan and B. H. Suits[1]

Physics Department, Michigan Technological University, Houghton, Michigan 49931-1295

Received October 6, 1998; revised January 26, 1999

Unlike NMR imaging, where only the components of the magnetic field gradients along the main applied field need be considered, all nonzero components of the gradients must be considered for NQR imaging of powder or polycrystalline materials. Any physically realizable gradient coil will have at least two nonzero components. Since the nonzero components are of comparable magnitude, image reconstruction will not be as straightforward as is found for NMR imaging. Here a practical NQR imaging reconstruction technique based on the use of standard techniques but using a nonrectilinear grid is demonstrated for physically realizable gradients. A two-dimensional image constructed using the ^{35}Cl NQR signal from a polycrystalline sample of $NaClO_3$ is presented to demonstrate the technique. © 1999 Academic Press

Key Words: **NQR imaging; image reconstruction; gradient coils.**

INTRODUCTION

Nuclear quadrupole resonance (NQR) imaging techniques, analogous to those used for NMR, have the advantage of requiring no large external magnetic field. In addition, the much larger sensitivity of the NQR frequency to the environment surrounding the nucleus used allows users of NQR to easily discriminate between different chemical environments. However, several complications arise for NQR imaging, and the direct application of the imaging techniques used for NMR is not possible.

Several groups have reported NQR imaging techniques (*1–14*) with varying degrees of success. In each of these studies, a simple magnetic field gradient that varies linearly in one spatial dimension is assumed either explicitly or implicitly. Unfortunately, such a gradient cannot be produced in practice without violating Maxwell's equations. In a previous paper (*15*) this difficulty was pointed out and a rather complicated way to get around it was proposed. Here we develop a much simpler method based solely on nutation spectroscopy, sometimes referred to as rotating-frame NQR imaging, but using a physically realizable gradient field from the start. The use of nutation spectroscopy for NQR imaging by itself is not new, and some of the basic ideas for image reconstruction with real gradients that are presented here may well apply to other NQR imaging methods.

[1] To whom correspondence should be addressed.

Below we discuss the theory and show that the effects of the additional components of the gradient field can be handled by an appropriate choice of coordinates combined with standard image reconstruction techniques. Image reconstruction in that coordinate system is then relatively straightforward. The reconstruction is demonstrated using the ^{35}Cl NQR signal from a polycrystalline sample of sodium chlorate ($NaClO_3$).

THEORY

The discussion here is limited to the use of an RF gradient coil constructed from a Maxwell pair with its axis along the z-direction, a commonly used configuration. Similar procedures can be used for other gradient coil configurations. It is assumed that the same gradient coil is used for both excitation and detection of the signal. Near the center of the coil, the RF field is given by

$$\begin{aligned}\boldsymbol{B}_1 &= G_{zz}z\hat{\boldsymbol{z}} + (G_{xx}x\hat{\boldsymbol{x}} + G_{yy}y\hat{\boldsymbol{y}}) \\ &= G_{zz}\left[z\hat{\boldsymbol{z}} - \frac{1}{2}(x\hat{\boldsymbol{x}} + y\hat{\boldsymbol{y}})\right]. \end{aligned} \quad [1]$$

A small volume element dV of the sample at (x, y, z) will experience an RF field of magnitude

$$|B_1| = G_{zz}(z^2 + 0.25(x^2 + y^2))^{1/2} \quad [2]$$

along a direction z' that is easily determined. If the RF field is applied for a time τ and then turned off, a time-dependent magnetization from the nuclei at (x, y, z) along the direction z' will result, where

$$M(t) \propto f(|B_1|\tau)\rho(x, y, z)\sin(\omega_Q t)dV \quad [3]$$

and where $\rho(x, y, z)$ is the density of NQR nuclei, $f(|B_1|\tau)$ describes the nutation of the nuclei during the RF pulse, and ω_Q is the NQR frequency. Relaxation processes have been neglected for simplicity. An EMF $s(t, \tau)$ will be induced in the coil as a result of the time-dependent magnetization. The coil sensitivity is proportional to $|B_1|$ because of reciprocity and the

1090-7807/99 $30.00

fact that $M(t)$ for an NQR measurement of a powder will be along $\boldsymbol{B}_1$; thus,

$$s(t, \tau) \propto |B_1|\omega_Q f(|B_1|\tau)\rho(x, y, z)\cos(\omega_Q t)dV. \quad [4]$$

The amplitude of the signal from the small volume element is then given by

$$s(\omega_Q, \tau) \propto |B_1| f(|B_1|\tau)\rho(x, y, z)dV. \quad [5]$$

Note that nuclei at the origin will not be excited and will not produce a signal; hence, the sample should be placed away from the origin. We also note here that the expression becomes significantly more complicated if a gradient coil is used for excitation and a solenoidal coil (e.g., along z) is used for signal reception (or vice versa); however, in that case no signal is observed for all nuclei in the x–y plane and a method based on a plane with zero signal similar to that proposed by Lee and Butler (*10*) could be used.

At this point it is useful to change to a more convenient coordinate system where $|B_1|$ depends on only one coordinate. For the Maxwell coil, a convenient choice is

$$\sigma = \sqrt{z^2 + 0.25(x^2 + y^2)}$$
$$\xi = \tan^{-1}\left(\frac{\sqrt{x^2 + y^2}}{2z}\right)$$
$$\phi = \tan^{-1}\left(\frac{y}{x}\right), \quad [6]$$

which are distorted spherical coordinates.

To simplify the discussion that follows, we consider a thin sample in the x–z plane for which the two-dimensional volume element is $dV = \frac{1}{2}\,\sigma\, d\sigma\, d\xi$. A projection of this sample is given by

$$p(\sigma) = \frac{1}{2}\int_{-\pi/2}^{\pi/2} \sigma\rho(\sigma, \xi)d\xi, \quad [7]$$

and the signal at ω_Q from the entire sample is then given by

$$S(\omega_Q, \tau) \propto \int_0^\infty \sigma f(\sigma\tau)\, p(\sigma)d\sigma, \quad [8]$$

where the fact that $|B_1| \propto \sigma$ has been used and the function f has been reexpressed in terms of σ.

The function f that describes the nutation of the nuclei for a powder averaged NQR signal is generally far more complicated than the simple sinusoidal dependence observed for NMR. For the $\pm\frac{3}{2}$ to $\pm\frac{1}{2}$ transitions of a nucleus with spin $I = \frac{3}{2}$ and asymmetry parameter $\eta = 0$, Bloom, *et al.* (*16*) have shown that we can write to a good approximation

$$f(\sigma\tau) \approx \frac{8}{3} J_1(\sqrt{3}\gamma G_{zz}\sigma\tau), \quad [9]$$

so that S is the first-order Hankel transform of p. Hence, in this case, the inversion is quite simple, and with σ expressed in units where $\sqrt{3}\ \gamma\ G_{zz}\ \sigma = 1$,

$$p(\sigma) \propto \int_0^\infty \tau S(\omega_Q, \tau)J_1(\sigma\tau)d\tau. \quad [10]$$

In other cases, this inversion may not be so straightforward and techniques such as the maximum entropy method can be employed (*8, 17*). The use of the Hankel transform for $I = \frac{3}{2}$ was previously proposed by Robert *et al.* (*8*).

To construct a two-dimensional image, projections are measured as the sample (or coil) is rotated, in this case about an axis parallel to the y-axis. Those projections are then appropriately weighted and combined to form an image. An explicit example of this using a simple algebraic reconstruction technique (ART) algorithm is presented below.

EXPERIMENTAL

Measurements

Measurements were performed for a compressed powder sample of $NaClO_3$ in the shape of a disk 4 mm in radius and 1 mm thick using a homebuilt spectrometer. The RF gradient coil used for both excitation and reception of the NQR signal consisted to two three-turn coils, 2.0 cm in diameter, spaced 1.6 cm apart. The coils were wound in the opposite sense to form a Maxwell pair (reversed Helmholtz). The center of the RF field (where $|B_1| = 0$) and the linearity of the gradient were determined using a small pick-up coil. The center of the sample was positioned away from the center of the coil so that none of the sample was located at the origin, and the axis of the sample was perpendicular to the coil axis. The coil was tuned and matched to 50 Ω. At the RF power levels used here, G_{zz} for this coil was measured to be 0.022 T/cm. Signals were measured for pulse lengths τ in 5 μs increments up to a maximum of 300 μs. Measurements were made at room temperature.

The measured free induction decays following the RF pulse were Fourier transformed to obtain the NQR intensity, $S(\omega_Q, \tau)$. The first-order Hankel transforms were performed using simple numerical integration.

Image Reconstruction

The data are collected in discrete, evenly space intervals of τ that, after transformation, result in a measure of $p(\sigma)$ at

discrete evenly space intervals of σ. The sample (or the coil) is rotated about the y-axis to obtain many other views of the sample. What is ultimately desired is an image obtained from those projections corresponding to the nuclear density, $\rho(x, z)$, in a form suitable for display.

To demonstrate image reconstruction, we use a modification of the additive algebraic reconstruction technique (AART) (*18, 19*). This method was chosen because of its simplicity. The $N \times N$ grid used for reconstruction is defined by

$$\begin{aligned} \sigma_k &= \sigma_0 + k\Delta\sigma, \quad k = 1, \ldots, N \\ \xi_l &= \xi_0 + l\Delta\xi, \quad l = 1, \ldots, N, \end{aligned} \tag{11}$$

where σ_0, $\Delta\sigma$, ξ_0, and $\Delta\xi$ are chosen to include the desired sample region with enough points to avoid a loss of resolution. This type of grid is illustrated in Fig. 1. The value of N was chosen to match the number of (discrete) evenly spaced values of $p(\sigma)$ to avoid an extra interpolation.

We designate our ith estimate of the image as $f_i\,(k, l)$. We can then compute a projection, p_i, based on this estimate,

$$p_i(\sigma_k) = \frac{1}{2}\sum_{l=1}^{N} \sigma_k f_i(\sigma_k, \xi_l)\,\Delta\sigma\Delta\xi, \tag{12}$$

which is compared to the measured projection (in our case obtained from the data with a discrete first-order Hankel transform) to generate the error e, which is used to correct the image estimate using

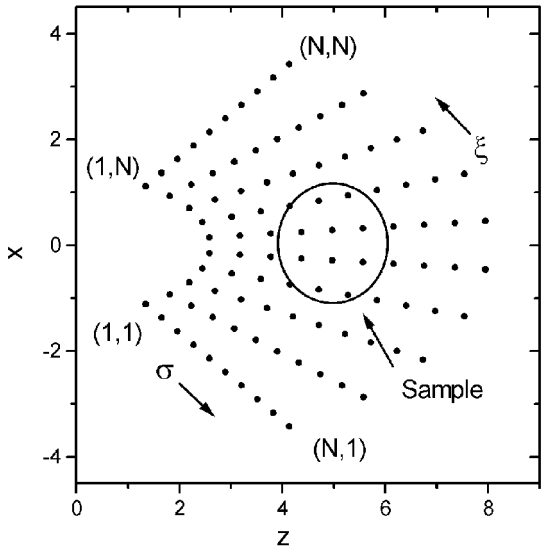

FIG. 1. A schematic showing grid points that can be used for (two-dimensional) image formation. A coarse grid is shown for clarity. These grid points are naturally derived from the form of the gradient field. The position and size of a hypothetical sample are shown for illustration.

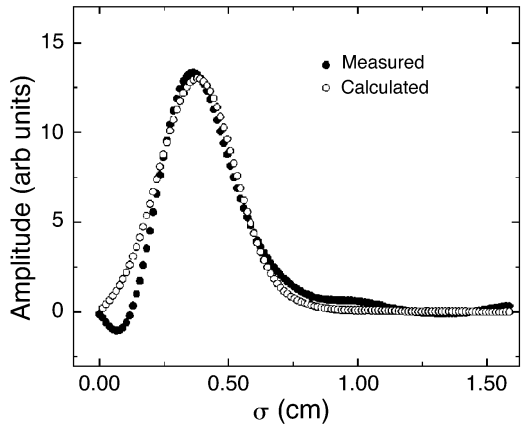

FIG. 2. Measured (closed circles) and numerically computed (open circles) projections for a 4 mm diameter thin disk lying in the x–z plane.

$$\begin{aligned} e(k) &= [p(\sigma_k) - p_i(\sigma_k)]/\sigma_k \\ f_{i+1}(k, l) &= \max\left[f_i(k, l) + \frac{c}{N}\, e(k),\, 0 \right], \end{aligned} \tag{13}$$

where the constant c, $0 < c \leq 1$, can be adjusted to aid convergence.

The sample is then rotated about the y-axis and a new projection is obtained.[2] At the same time, f_{i+1} is rotated by the same angle about the same axis. The rotation of f requires interpolation. (Alternatively, f could be held fixed; however, this makes the computation of the new p_i quite complicated.) For this new projection, e is calculated and the image estimate is adjusted as above. This process is continued until the changes in f become acceptably small. In practice, previously recorded projections for many different sample orientations are measured and are each reused several times. For display, the values of f are interpolated onto a rectilinear grid. We used an initial image estimate $f_0(k, l) = 0$.

RESULTS AND DISCUSSION

To simplify the experimental demonstration of image reconstruction, a thin circular sample was used with its axis along the y-direction and sample rotations were taken to be about that axis. Hence, an actual physical rotation is not necessary since projections from all angles would look the same.

Figure 2 shows the measured one-dimensional projection obtained after a first-order Hankel transform of the nutation data. Figure 2 also shows the results of a numerical calculation based on the size and position of our sample and the theory above (Eqs. [1]–[7]) with the same processing (zero fills, Gaussian apodization, etc.) as was used for the experimental

[2] In practice, one only needs to rotate through 180°; however, some experimental imperfections can be partially canceled if the rotation is done through the full circle.

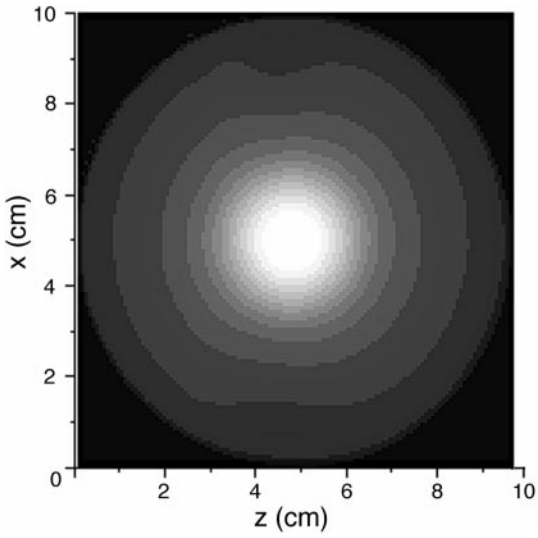

FIG. 3. A measured two-dimensional NQR image of a 4-mm diameter thin disk reconstructed using a (σ, ξ) grid with $N = 256$, and then interpolated onto a rectilinear (x, z) grid for display.

data. There is very good agreement between the two. The small negative dip in the experimental results has been traced to power amplifier droop that occurs for longer pulse lengths.

Figure 3 shows the output of the modified AART image algorithm using the measured one-dimensional projection and $N = 256$, showing an image that reasonably well represents the nuclear density in this sample.

It is worth commenting that in some circumstances the assumption that the B_1 field varies only in magnitude along a single direction may be a reasonable approximation. Consider the schematic situation shown in Fig. 1. Within the sample region, the grid points are almost rectilinear and regions outside the sample contribute no signal. Hence, a reasonable image could be made in that situation by simply using rectilinear coordinates and standard methods. However, that approximation is not generally valid, and such an approximation needs to be justified on a case-by-case basis.

CONCLUSION

A method for NQR imaging based on nutation spectroscopy and physically realizable RF gradient fields has been demonstrated for the first time. The method makes use of a new set of (nonrectilinear) coordinates during image reconstruction. The new set of coordinates is derived from the form of the gradient field, and the use of those coordinates simplifies reconstruction. An explicit reconstruction method using a modified additive arithmetic reconstruction technique (AART) was used to produce an image of a thin sample of $NaClO_3$ from ^{35}Cl NQR nutation measurements, demonstrating the feasibility of the imaging method.

REFERENCES

1. S. Matsui, K. Kose, and T. Inouye, *J. Magn. Reson.* **88,** 186 (1990).
2. E. Rommel, P. Nickel, R. Kimmich, and D. Pusiol, *J. Magn. Reson.* **91,** 630 (1991).
3. P. Nickel, E. Rommel, R. Kimmich, and D. Pusiol, *Chem. Phys. Lett.* **183,** 183 (1991).
4. E. Rommel, D. Pusiol, P. Nickel, and R. Kimmich, *Meas. Sci. Technol.* **2,** 866 (1991).
5. V. L. Ermakov, R. H. Kurbanov, D. Ya. Osokin, and V. A. Shagalov, *Appl. Magn. Reson.* **3,** 975 (1992).
6. E. Rommel, R. Kimmich, H. Robert, and D. Pusiol, *Meas. Sci. Technol.* **3,** 446 (1992).
7. Y. Lee, D. C. Michaels, and L. G. Butler, *Chem. Phys. Lett.* **206,** 464 (1993).
8. H. Robert, D. Pusiol, E. Rommel, and R. Kimmich, *Z. Naturforsch.* **49a,** 35 (1994).
9. P. Nickel, H. Robert, R. Kimmich, and D. Pusiol, *J. Magn. Reson. A* **111,** 191 (1994).
10. Y. Lee and L. G. Butler, *J. Magn. Reson. A* **112,** 92 (1995).
11. R. Kimmich, *Z. Naturforsch.* **51a,** 330 (1996).
12. H. Robert, and D. J. Pusiol, *Z. Naturforsch* **51a,** 353 (1996).
13. H. Robert, A. Minuzzi, and D. J. Pusiol, *J. Magn. Reson. A* **118,** 189 (1996).
14. H. Robert, and D. Pusiol, *J. Magn. Reson. A* **118,** 279 (1996).
15. B. H. Suits and G. Y. Plude, *J. Magn. Reson. A* **117,** 84 (1995).
16. M. Bloom, E. L. Hahn, and B. Herzog, *Phys. Rev.* **96,** 1699 (1955).
17. E. D. Laue, J. Skilling, J. Stauton, S. Sibisi, and R. Brereton, *J. Magn. Reson.* **62,** 437 (1985).
18. G. T. Herman, A. Lent, and S. Rowland, *J. Theor. Biol.* **42,** 1 (1973).
19. P. Gilbert, *J. Theor. Biol* **36,** 105 (1972).